C_n^2 profilometry from Shack-Hartmann data: model and experiment

J. Voyez[1a], C. Robert[1], B. Fleury[1], N. Védrenne[1], V. Michau[1], T. Fusco[1], and E. Samain[2]

[1] Office National d'Etudes et de Recherches Aérospatiales, BP 72, 92322 Châtillon, France
[2] Observatoire du Plateau de Calern, 06460 Caussols, France

Abstract. Wide Field Adaptive Optics (WFAO) systems require a precise reconstruction of the turbulent volume. The C_n^2 profile, representing the turbulence strength, becomes a critical parameter for the final tomographic reconstruction performance. We present a new method, CO-SLIDAR (COupled SLope and scIntillation Detection And Ranging), that uses correlations of slopes and scintillation indexes recorded on a Shack-Hartmann (SH), to retrieve the C_n^2 profile. A design is proposed for the instrument. Reconstruction performances are showed in simulation. Tests are carried out on the optical bench, and improvements are suggested. Sensitivity of the method to outer scale is demonstrated.

1 Introduction

The design phase for the WFAO systems for the ELTs has started. LTAO (ATLAS), MCAO (MAORY) and MOAO (EAGLE) systems have been studied for the E-ELT. All these systems have in common a need for a precise tomographic reconstruction of the turbulent volume. The impact of C_n^2 structure on WFAO performance has been studied in [1]. In that frame, getting of high-resolution C_n^2 profiles is then a crucial point for the design of the E-ELT AO systems.

In this context, we propose a new profilometry method, named CO-SLIDAR [2]. Taking advantage of correlations of slopes and scintillation indexes recorded simultaneously on a SH from a binary star, CO-SLIDAR leads to an accurate retrieval of the C_n^2 profile. It conjugates the sensibility to low altitude layers, with correlations of slopes, like a SLODAR [3], and the sensibility to high altitude layers, delivered by correlations of scintillation indexes, like SCIDAR [4] or MASS [5].

CO-SLIDAR has been validated in numerical simulations [2] and first-tested on real SH data, using a smart estimator to extract slopes and intensities [6]. The extension of the method to a single source has also been tested on infrared data [7]. The next step is a complete on-sky validation of the concept. In that perspective, we designed a full-dedicated 30×30 subapertures SH, that we set up on the 1.5 m MeO telescope, at the Observatoire de la Côte d'Azur, in South of France.

In section 2, we recall CO-SLIDAR theoretical background. In section 3, we present the design of the optical bench called ProMeO, for profilometry with MeO telescope. Technical choices are mainly made to get high resolution in altitude. The quality of C_n^2 reconstruction is shown in simulation. Tests performed throughout the first observation campaign are presented in 4. In section 5, we begin to investigate CO-SLIDAR sensitivity to outer scale L_0 by studying the inversion criterion value. Our conclusions and perspectives to improve the experiment are exposed in section 6.

2 Problem statement with SH slope and scintillation correlations

Given a star with position α in the field of view (FOV), a SH delivers a set of wavefront slopes and intensities per frame. The slope computed on the m^{th} subaperture focal image is a bi-dimensional vector $\mathbf{s}_m(\alpha)$ with two components $s_m^k(\alpha)$, along the k axis ($k \in \{x, y\}$). Star intensities, denoted $i_m(\alpha)$ and recorded in every subaperture m, lead to scintillation index $\delta i_m(\alpha) = \frac{i_m(\alpha) - o_m(\alpha)}{o_m(\alpha)}$ where $o_m(\alpha)$ is the time-averaged star intensity.

[a] juliette.voyez@onera.fr

In Rytov regime, meaning weak perturbations, turbulent layers contributions can been considered independent. Correlations of slopes and scintillation are then written as $C_n^2(h)$ integrals, weighted by functions, denoted W_{ss}^{kl} for slope correlations, W_{ii} for scintillation index correlations and W_{si}^{k} for correlations between slopes and scintillation indexes, which refers to coupling in the following. These functions are not detailed here, but their expressions depend on SH geometry, statistical properties of the turbulence, star separation θ, distance between subapertures $\mathbf{d}_{mn}$ and altitude h. These expressions are derived from the calculation of the terms of the anisoplanatism error described in [8].

Finally, for two stars separated from θ, slope correlations $\langle s_m^k s_n^l \rangle(\theta)$, scintillation index correlations $\langle \delta i_m \delta i_n \rangle(\theta)$ and their coupling $\langle s_m^k \delta i_n \rangle(\theta)$ are directly related to the C_n^2 profile by expressions 1 to 3:

$$\langle s_m^k s_n^l \rangle(\theta) = \int_0^{+\infty} C_n^2(h)\, W_{ss}^{kl}(h, \mathbf{d}_{mn}, \theta)\, dh, \tag{1}$$

$$\langle \delta i_m \delta i_n \rangle(\theta) = \int_0^{+\infty} C_n^2(h)\, W_{ii}(h, \mathbf{d}_{mn}, \theta)\, dh, \tag{2}$$

$$\langle s_m^k \delta i_n \rangle(\theta) = \int_0^{+\infty} C_n^2(h)\, W_{si}^{k}(h, \mathbf{d}_{mn}, \theta)\, dh. \tag{3}$$

Experimentally, correlations of SH data are estimated from a finite number of frames. They are then stacked in a single dimension covariance vector $\mathbf{C_{mes}}$. This vector is filled in with cross-correlations, collected in the two analysis directions, corresponding to the star separation θ, but also their autocorrelations, corresponding to the case $\theta = 0$. Layer contribution to $\mathbf{C_{mes}}$ have been discussed in [2]. We only recall that slope correlation are mainly sensitive to low altitude layers, while scintillation correlations are more sensitive to high altitude layers. It relates directly to C_n^2 in the problem statement as follows, assuming a discretized turbulence profile:

$$\mathbf{C_{mes}} = M\mathbf{C_n^2} + \mathbf{C_d} + \mathbf{u} \tag{4}$$

where M is the interaction matrix; $\mathbf{C_d}$ is the vector of correlations of measurement noises, including photon and detector noises. $\mathbf{u}$ represents uncertainties on $\mathbf{C_{mes}}$ due to the limited number of frames. The column vectors of M are formed by the concatenation of the weighting functions W.

Assuming the system is well calibrated, it is possible to completely determine $\mathbf{C_d}$ and define a non-biased estimation of the covariance vector, $\hat{\mathbf{C}}_{\mathbf{mes}} = \mathbf{C_{mes}} - \mathbf{C_d}$. This would make it possible to rewrite the direct problem:

$$\hat{\mathbf{C}}_{\mathbf{mes}} = MC_n^2 + \mathbf{u} \tag{5}$$

A sampled estimate of C_n^2, $\tilde{\mathbf{S}}$, is retrieved from the inversion of Eq. 5, assuming that the convergence noise $\mathbf{u}$ is Gaussian. For physical reasons C_n^2 is never negative, so $\tilde{\mathbf{S}}$ minimizes the maximum likelihood (ML) criterion J under positivity constraint:

$$J = (\hat{\mathbf{C}}_{\mathbf{mes}} - M\tilde{\mathbf{S}})^T C_{conv}^{-1} (\hat{\mathbf{C}}_{\mathbf{mes}} - M\tilde{\mathbf{S}}) \tag{6}$$

where $C_{conv} = \langle \mathbf{u}\mathbf{u}^T \rangle$ is the covariance matrix of $\mathbf{u}$, the convergence noise, due to the limited number of frames.

3 Design of the ProMeO experiment and performances in simulation

In this section we describe the design of the first ProMeO bench. The CO-SLIDAR instrument is mounted at the Coudé focus of the MeO telescope of the Observatoire de la Côte d'Azur, in South of France. The diameter of the telescope is $D = 1.5\ m$ and the central obscuration is 34 %. The Coudé train is afocal, composed of seven mirrors and one doublet. The beam of light has a diameter of $\Phi = 60\ mm$ at the output of the train. ProMeO optical diagram is shown in Fig. 1. Two lenses of focal lengths 800 mm and 56 mm are used to image the telescope pupil onto the 30×30 lenslet array. The microlenses have a pitch of 143 μm and a focal length of 3.4 mm. As it is too short to form an

image directly on the detector array, we use an additional pair of lenses to transfer the focal plane, with a magnification factor of 1.25. The camera used is an Andor iXon3 885 electron multiplication CCD (EMCCD). The detector is a 1000×1000 8 μm pixel array. The quantum efficiency (QE) at $\lambda = 0.55\,\mu m$ is about 50 %. The SH array having 30×30 subapertures, then the subaperture diameter is $d_{sub} = 5\ cm$.

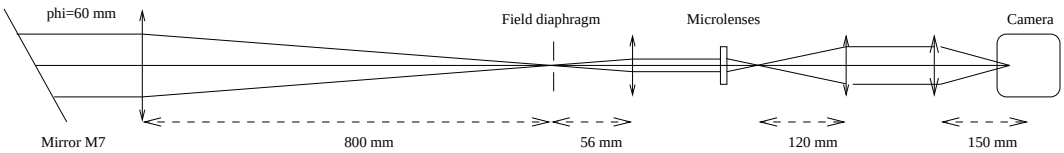

Fig. 1. The ProMeO optical bench.

Observations being performed at $\lambda = 0.55\ \mu m$, this leads to a pixel scale of 1.1 arsec/pixel at Shannon sampling. As we want to observe binary stars with separation $\theta \simeq 20$ arsec, the FOV in the subaperture is 25 arsec.

SH sizing is mainly brought about by altitude resolution and sensitivity to scintillation. Small subapertures bring high altitude resolution and high scintillation index as well without too much spatial averaging. The altitude resolution δh and the maximum sensing altitude H_{max} are obtained with simple geometrical rules using cross-correlations [3]:

$$\delta h = \frac{d_{sub}}{\theta} \tag{7}$$

$$H_{max} = \frac{D}{\theta} \tag{8}$$

This leads to $\delta h \simeq 500\ m$ and $H_{max} \simeq 15\ km$ for stars separated from 20 arsec. In principle, C_n^2 restoration above 15 km should be obtained using scintillation autocorrelations, as detailed in [2].

This 30×30 SH configuration has been tested in numerical simulations. Slope and intensity are computed after 100 wave propagations through 32 phase screens, representing 32 turbulent layers, simulating the complete electromagnetic field at the telescope pupil. As we perform 9 cuts on it at each propagation, we get 900 SH frames for further processing. Here we do no take into account measurement noises. The input outer scale L_0 is 8 m. The input profile and the result after CO-SLIDAR restoration are presented on Fig. 2. In this figure, we can see very good agreement between the true input profile and the C_n^2 restoration until 15 km, as expected. Layers under 5 km are reconstructed thanks to slope correlations, while both the plateau between 5 and 12 km and the layer at 15 km are reconstructed thanks to scintillation correlations. Therefore CO-SLIDAR retrieves an accurate C_n^2 profile from the ground to 15 km of altitude, with a resolution of about 500 m, using slope and scintillation cross-correlations. Nevertheless, the layers over 15 km are not so well reconstructed, but this difficulty can be explained below. For one layer at altitude h, the weighting function relative to the autocorrelation of scintillation (Eq. 2 with $\theta = 0$) has a full width at half maximum of about $\sqrt{\lambda h}$, the Fresnel radius [9]. This quantity decreases with decreasing altitude and for example, with $\lambda = 0.55\,\mu m$, $\sqrt{\lambda h} \simeq 10\ cm$ at $h = 20\ km$, $\sqrt{\lambda h} \simeq 7\ cm$ at $h = 10\ km$ and $\sqrt{\lambda h} = 0\ cm$ at ground level (*Cf.* Fig. 3). Knowing that the subaperture diameter is $d_{sub} = 5\ cm$, we have measurement points on the curve peak only for $d_{mn} = 0$ and 5 cm (respectively 0 and 1 in number of subapertures). Actually, we only have two points of measurement with strong signal, for high altitude layers, and this may be too low to get a good sensitivity from scintillation autocorrelation. An improvement of the sensitivity could be achieved using smaller subapertures, but this would lead to very low fluxes at subaperture level. An other solution would be to change the wavelength and work in the infrared domain.

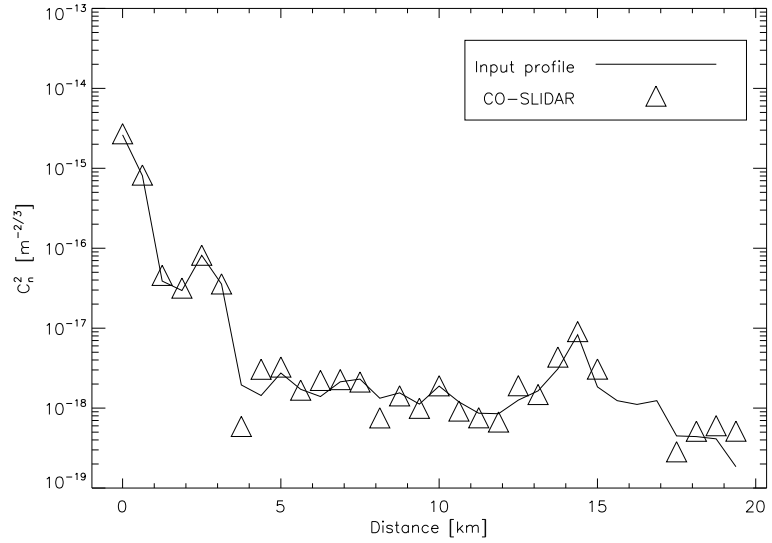

Fig. 2. Inversion results from CO-SLIDAR data, with 32 estimated layers.

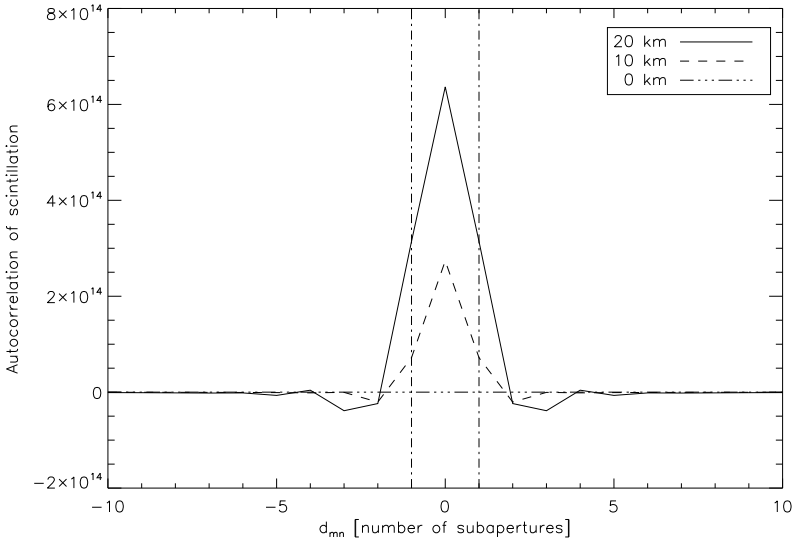

Fig. 3. Weighting functions relative to scintillation autocorrelation, for $h = 20\ km$ and $h = 10\ km$. Vertical lines represent $d_{mn} = -1$ and 1, in number of subapertures.

4 Returns on the first campaign: preliminary results

Several tests were performed on the ProMeO bench before coupling it with the MeO telescope. First, the EMCCD camera was fully characterized in lab in terms of linearity, gain and noise. A good agreement with constructor values was found. Then, we controlled the slope measurement linearity on the SH, to ensure that no distortion was induced by the focal plane transfer system. We formed the centered image of a point like source through the microlenses and we used it as a reference. Then, we made small displacements around the reference between -3 and 3 pixels. We checked the linearity between

the input slope and the one we measured on the detector. We found that the measurement is linear in the region of interest, defined by a square of 3×3 pixels^2 around the reference. The multiplying factor is close to 1 and the measurement variation between the subaperture at the center and at the edges of the SH does not exceed 0.1 pixel. This is weak, nevertheless, it is an instrumental response that can be fully calibrated in order to take it into account in the reconstruction process. Fig. 4 shows the results for a vertical slope measurement with the reference at the edge of the subaperture image. The SH was split into six rings, from the center to the edges, the first ring being at the center and the sixth ring at the edges.

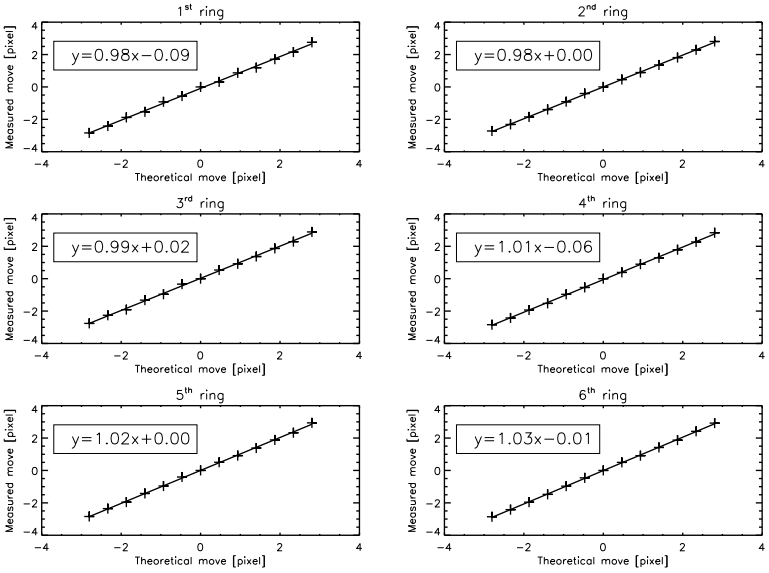

Fig. 4. Slope vertical measurements in different rings of the SH, for a reference at the edge of the subaperture image.

Second, we calibrated the transmission of the whole ProMeO and Meo telescope system. To do so we used a He-Ne laser at $\lambda = 543.5\ nm$. The Coudé train gives a global transmission of 32 %. The ProMeO bench transmission, obtained with the same method, is 75 %. The atmospheric transmission of the site being about 70 %, the full transmisson of the CO-SLIDAR instrument is $T_{total} = 17$ %. We also check the agreement between theoretical flux and measured flux, on a single star. We choose Vega, with $m_V = 0$ (see Fig. 5). The flux measurement is linear in the subaperture, but we can see that it is lower than the expected one. This point has to be studied to find out where the signal loss comes from.

Here we encounter one of the limitations of the experiment. As we want to freeze the turbulence, very short exposure times of a few milliseconds are mandatory. With a subaperture of 5 *cm* and such a transmission, the number of detected photons N_{ph} per subaperture and per frame is very limited. Table 1 summarizes this number N_{ph} for different visible magnitudes m_V and exposure times t_{exp}. Therefore, a compromise must be done between exposure time and signal to noise ratio (SNR). Indeed, with 80 $N_{ph}/sub/frame$, and assuming 4 pixels in the image spot, this leads to 20 N_{ph} per pixel, and a $SNR \simeq 4.5$, decreasing to $SNR \simeq 3.5$ with 50 $N_{ph}/sub/frame$. We also see that with this 30×30 SH configuration, stars with magnitude larger than $m_V = 5$ will not be available for the experiment, as they produced too few detectable photons, then reducing the sky coverage.

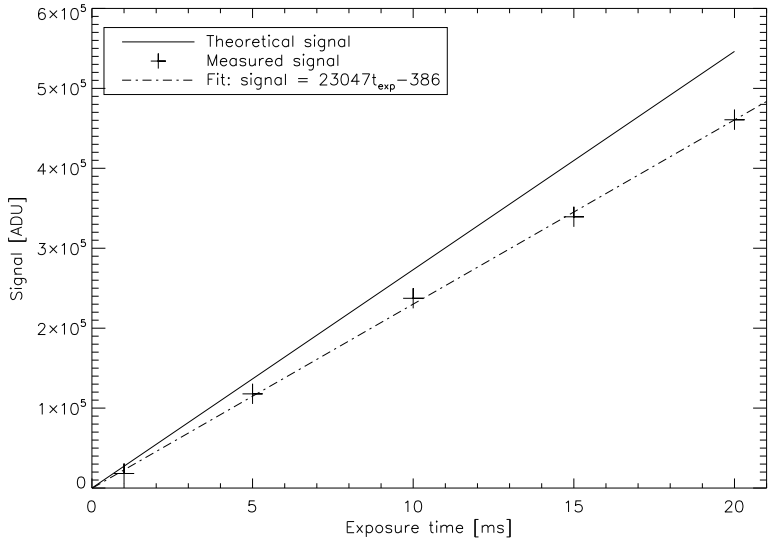

Fig. 5. Control of signal measurement at subaperture level, on Vega, $m_V = 0$.

m_V	t_{exp} (ms)	$N_{ph}/sub/frame$
3	1	134
	3	402
	5	671
4	1	53
	3	160
	5	267
5	1	21
	3	63
	5	106
6	1	8
	3	25
	5	42

Table 1. Number of detected photons N_{ph} per subaperture and per frame for different visible magnitudes and exposure times.

5 CO-SLIDAR sensitivity to outer scale

As the outer scale L_0 will be a parameter of interest for the ELTs, we began to investigate its possible retrieval with CO-SLIDAR, taking advantage of the telescope large diameter. The first step of this work is to study in simulation the method sensitivity to L_0. Simulations with a 30×30 SH being very heavy to run, we perform them on downscaled cases. We do again wave propagations throughout phase screens, to simulate 2000 frames of SH data, for which slopes and intensities are computed. The SH has 16×16 subapertures on a 40 *cm* telescope, so that the subaperture diameter is 2.5 *cm*. The input L_0 for data simulation is 1.25 *m*. The input C_n^2 profile is the same as in section 3. We study the CO-SLIDAR reconstruction for different L_0, between 0.5 *m* and 10 *m*. We represent the ML criterion minimum (see Eq. 6) for the given L_0 on Fig. 6.

As we can see, the minimum of the ML criterion J is for the true L_0, confirming that CO-SLIDAR is sensitive to outer scale. This goes in the way of a combined determination of the C_n^2 and the L_0 profiles, using relations proposed in [10] and [11]:

$$C_n^2 = aML_0^{\frac{4}{3}} \tag{9}$$

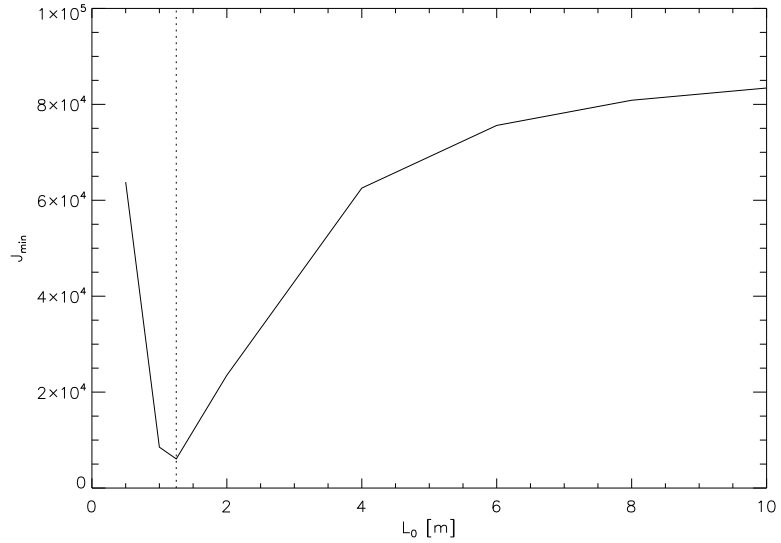

Fig. 6. Minimum of the ML criterion J for different L_0 values. The dashed vertical line represents $L_0 = 1.25$ *m*.

where a is a constant, and M, the gradient of potential refractive index, is given by:

$$M = -\left(\frac{78 \times 10^{-6} p}{T}\right) \frac{\delta \ln \theta}{\delta Z}. \tag{10}$$

with θ the potential temperature and Z the vertical coordinate. T and p respectively stand for temperature and pressure.

6 Conclusions and perspectives

In this paper we presented the CO-SLIDAR method to retrieve the C_n^2 profile with a SH, using the information provided by both slope and intensity data. We proposed a design for the instrument and we showed its performances in simulation. We have made a 30×30 subaperture SH having a FOV of 25 arsec to observe binary stars. The profile is reconstructed in simulation from the ground to 20 *km* of altitude, with a 500 *m* altitude resolution. We also demonstrated that CO-SLIDAR is sensitive to outer scale. Combined determination of the two parameters must now be studied.

The tests on the ProMeO bench highlighted some limitations of this optical configuration. This leads to the preparation of a new SH design, increasing the subaperture diameter to get more flux. Additional experimentation in lab is planned, to optimize optical settings. The optical transmission of the Coudé train is going to be improved. Another observation campaign is being prepared, with this time records of SH data on binary stars, in order to estimate the C_n^2 profile of the site.

This work is in progress with a plan of simulations. Detection noises must be taken into account. Different SH geometries have to be compared. The accuracy and the toughness of the reconstruction process should be estimated on different C_n^2 profiles by defining a dedicated metric. The impact of the convergence noise due to the finite number of frames should be quantified.

7 Acknowledgments

This work has been performed in the framework of a Ph.D thesis supported by Onera, the French Aerospace Lab, and the French Direction Générale de l'Armement (DGA). The authors are very grateful to the team operating at MeO station, for the use of the 1.5 m telescope and their help and support throughout the whole campaign.

References

1. T. Fusco and A. Costille. Impact of Cn2 profile structure on wide-field AO performance. In *Society of Photo-Optical Instrumentation Engineers (SPIE) Conference Series*, volume 7736 of *Society of Photo-Optical Instrumentation Engineers (SPIE) Conference Series*, July 2010.
2. N. Védrenne, V. Michau, C. Robert, and J.-M. Conan. Cn2 profile measurement from shack-hartmann data. *Opt. Lett.*, 32(18):2659–2661, September 2007.
3. R. W. Wilson. SLODAR: measuring optical turbulence altitude with a Shack-Hartmann wavefront sensor. *Mon. Not. R. Astron. Soc.*, 337:103–108, November 2002.
4. A. Fuchs, M. Tallon, and J. Vernin. Focusing on a Turbulent Layer: Principle of the "Generalized SCIDAR". *Publ. Astron. Soc. Pac.*, 110:86–91, January 1998.
5. V. Kornilov, A. A. Tokovinin, O. Vozyakova, A. Zaitsev, N. Shatsky, S. F. Potanin, and M. S. Sarazin. MASS: a monitor of the vertical turbulence distribution. In P. L. Wizinowich & D. Bonaccini, editor, *Society of Photo-Optical Instrumentation Engineers (SPIE) Conference Series*, volume 4839 of *Society of Photo-Optical Instrumentation Engineers (SPIE) Conference Series*, pages 837–845, February 2003.
6. C. Robert, J. Voyez, N. Védrenne, and L. Mugnier. Cn2 profile from Shack-Hartmann data with CO-SLIDAR data processing. *ArXiv e-prints*, January 2011.
7. N. Védrenne, A. Bonnefois Montmerle, C. Robert, V. Michau, J. Montri, and B. Fleury. Cn2 profile measurement from Shack-Hartmann data: experimental validation and exploitation. In *Society of Photo-Optical Instrumentation Engineers (SPIE) Conference Series*, volume 7828 of *Presented at the Society of Photo-Optical Instrumentation Engineers (SPIE) Conference*, October 2010.
8. C. Robert, J.-M. Conan, V. Michau, T. Fusco, and N. Védrenne. Scintillation and phase anisoplanatism in Shack-Hartmann wavefront sensing. *Journal of the Optical Society of America A*, 23:613–624, March 2006.
9. J. Vernin and M. Azouit. Image processing adapted to the atmospheric speckle. II. Remote sounding of turbulence by means of multidimensional analysis. *Journal of Optics*, 14:131–142, 1983.
10. V. I. Tatarskii. *The effects of the turbulent atmosphere on wave propagation*. 1971.
11. C. E. Coulman, J. Vernin, Y. Coqueugniot, and J.-L. Caccia. Outer scale of turbulence appropriate to modeling refractive-index structure profiles. *Appl. Opt.*, 27:155, January 1988.